박판단면의 비선형 좌굴거동에 관한 해석적연구

A Study on the Nonlinear Buckling Behavior of Thin-Walled Sections

진 창 선[1] · 권 영 봉[2]
Jin, Chang Sun Kwon, Young Bong

요 약 : 본 논문에서는 박판구조물의 좌굴모드 및 좌굴응력값을 구하기 위해서 spline finite strip method를 이용하여 박판구조물이 흔히 좌굴을 일으키기 전에 다양한 초기부정형으로 인하여 발생할 수 있는 전좌굴변형 및 비선형 응력-변형률 관계를 포함한 비선형 비탄성 좌굴해석프로그램을 개발하였다. 이 방법은 다양한 지점조건과 임의의 하중조건을 가지는 박판구조물에 적용이 가능하며, 초기부정형과 잔류응력을 포함하고 있는 다양한 형태의 박판구조물의 비선형 좌굴거동을 보다 정확하게 예측할 수가 있었다.

ABSTRACT : The purpose of this paper is to provide and verify an analytical method, based on the spline finite strip method, which can be used to investigate the buckling mode and stress of thin-walled steel sections. Geometric imperfection and initial stress of plates and plate assemblies, which are resulted from various preloadings and may cause prebuckling deformations before buckling, are included in the analysis. Material nonlinearity and residual stress are also considered. It can be applied to sections with simple or non-simple boundary conditions and arbitrary loading. The method has been applied to investigate the buckling behavior of plates and plate assemblies which are subjected to compression with initial imperfections and residual stresses.

핵 심 용 어 : 박판단면, B_3-유한대판법, 초기변형, 전좌굴변형, 잔류응력, 재료비선형, 비선형좌굴

KEYWORDS : thin-walled section, B_3-spline finite strip method(SFSM), initial imperfection, prebuckling deformation, residual stress, material nonlinearity, nonlinear buckling

1) 영남대학교 공업기술연구소, 연구원
2) 정회원, 영남대학교 토목공학과 부교수, 공학박사

본 논문에 대한 토의를 1999년 3월 31일까지 학회로 보내주시면 토의 회답을 게재하겠습니다.

1. Introduction

Thin-walled sections may have pre-buckling deformations due to geometric imperfections and initial strains before buckling in a local, a distortional or an overall mode(Kwon 1993, Hancock 1978). In the post-buckling range, the buckling mode may change into a different buckling mode near second bifurcation point. The purpose of this paper is to provide and verify an analytical method, based on the spline finite strip method, which can be used to investigate the buckling modes and stresses of thin-walled structures which have geometric imperfections and initial strains and may have prebuckling deformations before buckling.

The method can be extended further to the second buckling analysis of pre-buckled structures considering complicated stresses and deformations in the post-buckling range. The spline finite strip method developed by Fan(1982) has been applied to the elastic and inelastic buckling analysis of thin-walled sections by Lau and Hancock(1990) and proven to be accurate and efficient.

However, the researches did not include the analysis of the imperfect structures which have initial imperfections and locked-in residual stresses. The structures may show first prebuckling deformations apart from the buckling mode and then may buckle into the primary mode(Pi 1992). The behavior may be significantly different from that of the perfect structures. In this paper, the basic B_3-spline function (Carl de Boor 1978) is adopted because of it's localized nature and hence it's ability to reduce the computing time by band-width mini-mization.

To take into account the nonlinear stress-strain properties of the material, several proposed stress-strain curves are considered in this paper. Numerical and algebraic integrations have jointly been performed for the stiffness matrix to improve the versatility.

It can be applied to sections which have simple or non-simple boundary conditions and are subjected to arbitrary loading. It is also unrestricted by the overall structural length.

2. Spline Finite Strip Analysis

2.1 Spline Function

A typical strip with section knots and a local coordinate system is shown in Fig. 1. In the spline finite strip method, the prismatic member is discretized by using n nodal lines in the transverse direction (*y-axis*) and m sections in the longitu-

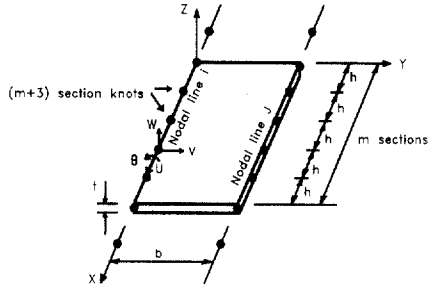

Fig. 1 A B_3-spline strip

dinal direction(x-*axis*). The two additional section knots on each nodal line are required to define the spline function over the length of a strip. Each section knot has four degrees of freedom, two out-of-plane deformations $w, \theta\,(=\partial w/\partial y)$ and two in-plane displacements u, v.

The spline function for displacement along the nodal line is the B_3-spline with m equal section lengths. The displacement function describing the longitudinal variation is taken as the summation of local B_3-splines by

$$f(x)=\sum_{i=-1}^{m+1} a_i \Phi_i(x) \qquad (2.1)$$

where $\Phi_i(x)$ is a local spline function as shown in Fig. 2(a) and a_i is a coefficient to be determined in the analysis. A linear combination of local B_3-splines is shown in Fig. 2(b). A local B_3-spline function is a piecewise cubic polynomial which is twice differentiable. A standard local B_3-spline function is defined by where h is section length shown in Fig. 2(a).

A set of splines amended for particular boundary conditions is shown on Fig. 2(c).

2.2 Displacement Function

The displacement functions are given by

$$\Phi_i(x)=\frac{1}{6h^3}\begin{cases}(x-x_{i-2})^3 & x_{i-2}\le x\le x_{i-1}\\ h^3+3h^2(x-x_{i-1})+3h(x-x_{i-1})^2-3(x-x_{i-1})^3 & x_{i-1}\le x\le x_i\\ h^3+3h^2(x_{i+1}-x)+3h(x_{i+1}-x)^2-3(x_{i+1}-x)^3 & x_i\le x\le x_{i+1}\\ (x_{i+2}-x)^3 & x_{i+1}\le x\le x_{i+2}\\ 0 & \text{otherwise}\end{cases} \qquad (2.2)$$

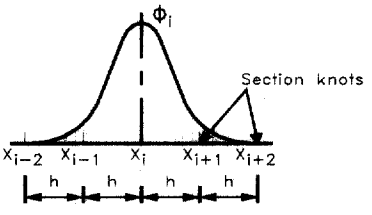

(a) A local B3-spline spline

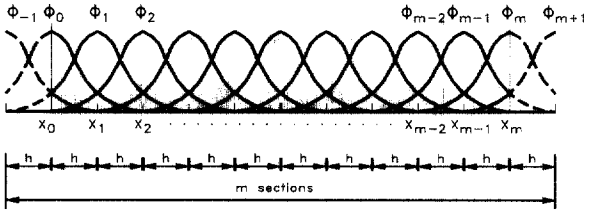

(b) A linear combination of local B3-splines

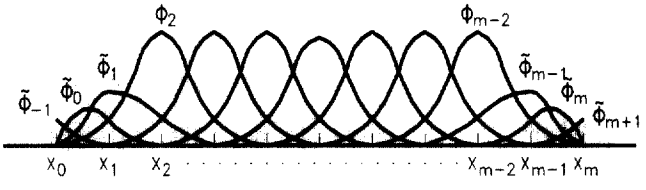

(c) Amended boundary local splines

Fig. 2 B3-splines

the product of the longitudinal B3-spline function and the transverse interpolation function.

In-plane strip displacements(u, v) in local coordinate system are expressed as

$$\begin{bmatrix} u \\ v \end{bmatrix} = [N_M][\Phi_M][\delta_M]$$

$$= \begin{bmatrix} N_1 & 0 & N_2 & 0 \\ 0 & N_1 & 0 & N_2 \end{bmatrix} \begin{bmatrix} [\Phi_1] & 0 & 0 & 0 \\ 0 & [\Phi_2] & 0 & 0 \\ 0 & 0 & [\Phi_3] & 0 \\ 0 & 0 & 0 & [\Phi_4] \end{bmatrix} \begin{bmatrix} u_i \\ v_i \\ u_j \\ v_j \end{bmatrix} \tag{2.3a}$$

where

$$\begin{aligned} N_1 &= 1 - \bar{y} \\ N_2 &= \bar{y} \\ \bar{y} &= \frac{y}{b} \end{aligned} \tag{2.3b}$$

in which b is the width of strip. $[\Phi_1] - [\Phi_4]$ are row matrices and each is composed of (m+3) B3-spline functions as defined by

$$\Phi = [\ \tilde{\Phi}_{-1},\ \tilde{\Phi}_0,\ \tilde{\Phi}_1,\ \Phi_2,\ \ldots,\ \Phi_{m-2},\ \tilde{\Phi}_{m-1},\ \tilde{\Phi}_m,\ \tilde{\Phi}_{m+1}] \tag{2.4}$$

where $\tilde{\Phi}$ indicates an amended boundary spline. The displacement coefficient vectors $[u_i], \ldots, [v_j]$ are column vectors and each has $(m+3)$ terms which correspond with those in Eq. 2.5.

Vector $[u_i]$ is defined as

$$[u_i] = [\ u_{-1},\ u_0,\ u_1,\ \ldots,\ u_{m-1},\ u_m,\ u_{m+1}\ ]^T \tag{2.5}$$

Out-of-plane strip displacement w is given in Eq. 2.6(a).

$$\begin{aligned} w &= [N_F][\Phi_F][\delta_F] \\ &= [N_3\ N_4\ N_5\ N_6] \\ &\times \begin{bmatrix} [\Phi_5] & 0 & 0 & 0 \\ 0 & [\Phi_6] & 0 & 0 \\ 0 & 0 & [\Phi_7] & 0 \\ 0 & 0 & 0 & [\Phi_8] \end{bmatrix} \begin{bmatrix} w_i \\ \theta_i \\ w_j \\ \theta_j \end{bmatrix} \end{aligned} \tag{2.6a}$$

where

$$\begin{aligned} N_3 &= 1 - 3\bar{y}^2 + 2\bar{y}^3 \\ N_4 &= y(1 - 2\bar{y} + \bar{y}^2) \\ N_5 &= 3\bar{y}^2 - 2\bar{y}^3 \\ N_6 &= y(\bar{y}^2 - \bar{y}) \end{aligned} \tag{2.6b}$$

$[\Phi_5] - [\Phi_8]$ are row matrices and each has (m+3) local B3-spline functions as defined by Eq. 2.4.

2.3 Strain-Displacement Relations

Both in-plane and out-of-plane displacements are considered in the nonlinear strain-displacement relations since membrane and plate bending problems may be coupled and therefore cannot be dealt with separately.

The strains in the plate at mid-surface are given by Novozhilov(1953)

$$\{\varepsilon\} = \begin{Bmatrix} \varepsilon_x \\ \varepsilon_y \\ \gamma_{xy} \end{Bmatrix} = \begin{bmatrix} \frac{\partial u}{\partial x} \\ \frac{\partial v}{\partial y} \\ \frac{\partial u}{\partial y} + \frac{\partial v}{\partial x} \end{bmatrix}$$

$$+\begin{bmatrix} \frac{1}{2}\left(\frac{\partial u}{\partial x}\right)^2+\frac{1}{2}\left(\frac{\partial v}{\partial x}\right)^2+\frac{1}{2}\left(\frac{\partial w}{\partial x}\right)^2 \\ \frac{1}{2}\left(\frac{\partial u}{\partial y}\right)^2+\frac{1}{2}\left(\frac{\partial v}{\partial y}\right)^2+\frac{1}{2}\left(\frac{\partial w}{\partial y}\right)^2 \\ \left(\frac{\partial u}{\partial x}\right)\left(\frac{\partial u}{\partial y}\right)+\left(\frac{\partial v}{\partial x}\right)\left(\frac{\partial v}{\partial y}\right)+\left(\frac{\partial w}{\partial x}\right)\left(\frac{\partial w}{\partial y}\right) \end{bmatrix} \tag{2.7}$$

The curvature-displacement relations are taken in the linear terms.

Eq. 2.7 are expressed as Eq. 2.8 in the condensed form.

$$\{\varepsilon\} = \left[[B_L] + \frac{1}{2}[B_N(d)]\right]\{d\} \tag{2.8}$$

where $[B_L]$ denotes the linear matrix and $[B_N(d)]$ is a nonlinear matrix which is a function of the displacement.

3. Nonlinear Stress-Strain Relations

3.1 Stress-Strain Relations

In the elastic range, the membrane stress-strain relations are given by

$$\begin{Bmatrix} \sigma_x \\ \sigma_y \\ \tau_{xy} \end{Bmatrix} = \begin{bmatrix} \frac{E}{1-\nu^2} & \frac{\nu E}{1-\nu^2} & 0 \\ \frac{\nu E}{1-\nu^2} & \frac{E}{1-\nu^2} & 0 \\ 0 & 0 & \frac{E}{2(1+\nu)} \end{bmatrix} \begin{Bmatrix} \varepsilon_x \\ \varepsilon_y \\ \gamma_{xy} \end{Bmatrix} \tag{3.1}$$

In the inelastic range, the incremental stress-strain relations for the case of uniform compression in the longitudinal direction can be expressed by

$$\begin{Bmatrix} d\sigma_x \\ d\sigma_y \\ d\tau_{xy} \end{Bmatrix} = \begin{bmatrix} D_x & D_1 & 0 \\ D_1 & D_y & 0 \\ 0 & 0 & D_{xy} \end{bmatrix} \begin{Bmatrix} d\varepsilon_x \\ d\varepsilon_y \\ d\gamma_{xy} \end{Bmatrix} \tag{3.2a}$$

which can be represented in matrix notation by

$$\{d\sigma\} = [D_M]_P\{d\varepsilon\} \tag{3.2b}$$

Similar to Eq. 3.1(c), the change in bending and twisting moment in a plate can be given in relation with the change of curvature.

$$\{dM\} = [D_F]_P\{d\rho\} \tag{3.2c}$$

$$[D_F]_P = \frac{t^3}{12}[D_m]_p \tag{3.2d}$$

The matrices $[D_M]_P$ and $[D_F]_P$ are the plastic property matrices describing the membrane and flexural displacements respectively.

3.1.1 Flow Theory of Plasticity

According to the flow theory of plasticity as formulated by Handelman and Prager, the material property coefficients in the inelastic range, D_x, D_1, D_y and D_{xy} are given by

$$D_x = \frac{x+3}{\Omega} \tag{3.3a}$$

$$D_y = \frac{4x}{\Omega} \tag{3.3b}$$

$$D_1 = \frac{2(x-1+2\nu)}{\Omega} \quad (3.3c)$$

$$D_{xy} = G = \frac{E}{2(1+\nu)} \quad (3.3d)$$

$$\Omega = \frac{x(5-4\nu)-(1-2\nu)^2}{E} \quad (3.3e)$$

$$x = \frac{E}{E_t} \quad (3.3f)$$

where E_t is the tangent modulus determined from the stress-strain curve of the material, and ν is the elastic value of Poisson's ratio. It should be noted that if $x=1$, i.e $E = E_t$, is substituted into Eq. 3.3(f), then $[D]_P$ is exactly same as $[D]_e$.

3.1.2 Deformation Theory of Plasticity

Inelastic plate buckling problems have been investigated by Bijlaard, Stowell and Ilyushin with the stress-strain relations based on the deformation theory of plasticity. Bijlaard and Stowell assumed continuous loading across the thickness of plate when buckling occured, whereas Ilyushin assumed the concept of strain reversal on the convex side of the plate. Test results agreed better with the analysis of Bijlaard, therefore his analysis is summarized in this section.

The material property moduli according to Bijlaard are given by

$$D_x = \frac{x+3+3e}{\Omega} \quad (3.4a)$$

$$D_y = \frac{4x}{\Omega} \quad (3.4b)$$

$$D_1 = \frac{2(x-1+2\nu)}{\Omega} \quad (3.4c)$$

$$D_{xy} = \frac{E}{2(1+\nu)+3e} \quad (3.4d)$$

$$\Omega = \frac{x(5-4\nu+3e)-(1-2\nu)^2}{E} \quad (3.4e)$$

$$e = \frac{E}{E_s} - 1 \quad (3.4f)$$

where E_s is the secant modulus determined from the stress-strain curve of the material, ν is the elastic value of Poisson's ratio and x is as defined in Eq. 3.3(f).

3.2 Stress-Strain Curve

In order to determine the values of the tangent and secant modulus at different stress levels, nonlinear material stress-strain curves have been represented in the forms of formulae.

3.2.1 Plank

According to Plank(1974), stress-strain curve can be represented by

$$\varepsilon = \frac{\sigma}{E}\frac{1-c\mu}{1-\mu} \quad (3.5a)$$

$$\frac{d\sigma}{d\varepsilon} = \frac{E(1-\mu)^2}{1-2c\mu+c\mu^2} \quad (3.5b)$$

where $\mu = \sigma/\sigma_y$ and c is a constant. A value of c=0.997 has been suggested

for the structural steel. Fig. 3 shows the effects of the c values on the shapes of the stress-strain curves determined using Eq. 3.5(a) and 3.5(b). E = 2.05 x 105MPa and σy = 320MPa have been used in Fig. 3.

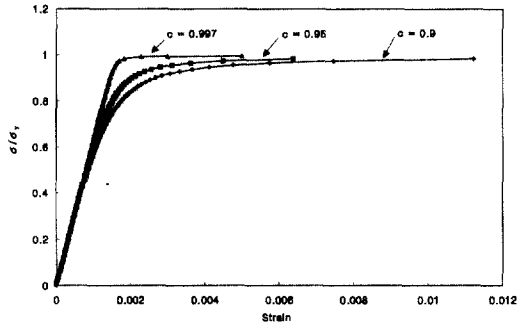

Fig. 3 Stress-Strain curves according to Plank

3.2.2 Ramberg-Osgood

The general form of the Ramberg-Osgood(1943) formula is expressed as

$$\varepsilon = \frac{\sigma}{E} + k\left(\frac{\sigma}{E}\right)^n \qquad (3.6a)$$

where k and n are constants. Ramberg and Osgood(1943) have derived expressions for determining k and n, hence, Eq. 3.6(a) can be re-written as

$$\varepsilon = \frac{\sigma}{E} + \frac{3\sigma}{7E}\left(\frac{\sigma}{\sigma_{0.7}}\right)^{n-1} \qquad (3.6b)$$

$$\frac{d\sigma}{d\varepsilon} = \frac{E}{1 + \frac{3n}{7}\left(\frac{\sigma}{\sigma_{0.7}}\right)^{n-1}} \qquad (3.6c)$$

$$\text{where } n = 1 + \frac{\log(17/7)}{\log(\sigma_{0.7}/\sigma_{0.85})} \qquad (3.6d)$$

and the stresses $\sigma_{0.7}$ and $\sigma_{0.85}$ are determined from the stress-strain curve of the coupon test.

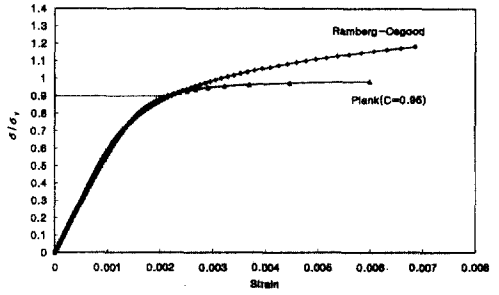

Fig. 4 Stress-Strain curve according to Ramberg-Osgood and Plank

They are the stresses corresponding to Es = 0.7E and Es = 0.85E respectively. The shape of the stress-strain curve determined using the Ramberg-Osgood formula is demonstrated in Fig. 4 and compared with Plank's formula where the yield stress and Young's modulus is the same as those used in Plank's formula.

3.2.3 Elastic-Perfectly Plastic Relations

Typically elastic-perfectly plastic curves for the mild steel shown in Fig. 5 are

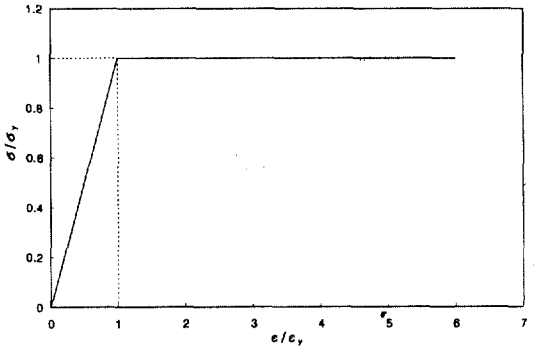

Fig. 5 Elastic-Perfectly Plastic Stress-Strain curve

generally adapted for the hot-rolled sections and built-up sections. The stress-strain relations follow the Hook's law and have a yield plateau. The curves are straight inclined with Young's modulus E up to yield stress and then horizontal with $E_t = 0$ neglecting the strain-hardening range.

4. Matrix Formulations for Nonlinear Buckling Analysis

4.1 Total Potential Energy

Total potential energy can be expressed as

$$\Pi = U + V \tag{4.1a}$$

where U is the strain energy and V is the potential energy. The strain energy can be expressed as

$$U = \int_v \{\varepsilon\}^T \{\sigma\}\, dv \tag{4.1b}$$

The potential energy of the applied membrane forces resulting from in-plane and out-of-plane buckling deformations are expressed as

$$V = \int_s \{d\}^T \{N\}\, ds \tag{4.2a}$$

where

$$\{N\}^T = \{N_x,\ N_y,\ N_{xy}\} \tag{4.2b}$$

and $\{d\}$ is the corresponding displacement vector.

The first variation of the total potential energy can be expressed as

$$\begin{aligned}\delta\Pi &= \delta(U+V) \\ &= \int_v \delta\{\varepsilon\}^T \{\sigma\} dv + \int_s \delta\{d\}^T \{N\}\, ds\end{aligned} \tag{4.3a}$$

where the first variation of the strain can be expressed as

$$\begin{aligned}\delta\{\varepsilon\} &= [B_L + B_N(d)]\,\delta\{d\} \\ &= [\bar{B}]\,\delta\{d\}\end{aligned} \tag{4.3b}$$

Since the linear terms in strain formulation disappear in the second variation, the second variation of the total potential energy can be given as

$$\begin{aligned}\frac{1}{2}\delta^2\Pi = &\frac{1}{2}\int_v \delta^2\{\varepsilon\}^T \{\sigma\} dv \\ &+ \frac{1}{2}\int_v \delta\{\varepsilon\}^T \delta\{\sigma\} dv\end{aligned} \tag{4.4a}$$

The second variation of the strain can be expressed as

$$\delta^2\{\varepsilon\} = \delta[B_N]\,\delta\{d\} \tag{4.4b}$$

The first term of the right side of Eq.4.4(a) is extended as

$$\begin{aligned}\frac{1}{2}\int_v \delta^2\{\varepsilon\}^T \{\sigma\} dv &= \int_v \delta\{d\}^T \delta[B_N]^T \{\sigma\} dv \\ &= \frac{1}{2}\int_v \delta\{d\}^T [G]^T [A]^T \begin{Bmatrix}\sigma_x \\ \sigma_y \\ \sigma_{xy}\end{Bmatrix} dv\end{aligned} \tag{4.5a}$$

and by the well known matrix property, Eq. 4.5(a) can be expressed as Eq. 4.5(b).

$$\frac{1}{2}\int_v \delta^2\{\varepsilon\}^T\{\sigma\}dv=\frac{1}{2}\int_v \delta\{d\}^T[K_\sigma]\delta\{d\}$$

$$=\frac{1}{2}\int_v \delta\{d\}^T[G]^T[\sigma]^T[G]\delta\{d\}dv \quad (4.5b)$$

where $[G]$ is a matrix defined in terms of the coordinates as expressed in Eq. 4.5(c)

$$[G]=\begin{bmatrix} N_1\Phi'_1 & 0 & N_2\Phi'_3 & 0 & 0 & 0 & 0 & 0 \\ 0 & N_1\Phi'_2 & 0 & N_2\Phi'_4 & 0 & 0 & 0 & 0 \\ 0 & 0 & 0 & 0 & N_3\Phi'_5 & N_4\Phi'_6 & N_5\Phi'_7 & N_6\Phi'_8 \\ N_1\Phi_1 & 0 & N_2\Phi_3 & 0 & 0 & 0 & 0 & 0 \\ 0 & N_1\Phi_2 & 0 & N_2\Phi_4 & 0 & 0 & 0 & 0 \\ 0 & 0 & 0 & 0 & N_3\Phi_5 & N_4\Phi_6 & N_5\Phi_7 & N_6\Phi_8 \end{bmatrix} \quad (4.5c)$$

$$[\sigma]=\begin{bmatrix} \sigma_x I_3 & \sigma_{xy} I_3 \\ \sigma_{xy} I_3 & \sigma_y I_3 \end{bmatrix}, \quad [I_3]=\begin{bmatrix} 1 & 0 & 0 \\ 0 & 1 & 0 \\ 0 & 0 & 1 \end{bmatrix} \quad (4.5d)$$

The second term of Eq. 4.4(a) is composed of conventional linear and nonlinear stiffness matrices and expressed as

$$\frac{1}{2}\int_v \delta\{\varepsilon\}^T\delta\{\sigma\}dv = \frac{1}{2}\int_v \delta\{d\}^T[\overline{B}]^T[D][\overline{B}]\delta\{d\}dv$$

$$=\frac{1}{2}\delta\{d\}^T[K]\delta\{d\}$$

$$=\frac{1}{2}\delta\{d\}^T([K_L]+[K_N])\delta\{d\} \quad (4.5e)$$

4.2 Formulations Including Prebuckling Deformations

At a point of equilibrium, the total potential energy is constant for infinitesimal buckling deformations; i.e. the first variation of the total potential energy equals zero. The critical condition for the buckling is that second variation of the total potential energy must be zero. This buckling criterion may be obtained from Eq. 4.5(a)-(e) as

$$\frac{1}{2}\delta^2\Pi = \frac{1}{2}\delta^2(U+V)$$

$$=\frac{1}{2}\delta\{d\}^T[K_T]\delta\{d\}=0 \quad (4.6a)$$

where $[K_T]$ is tangent stiffness matrix as given in Eq. 4.7 and expressed as

$$[K_T]=[K_L]+[K_N]+[K_\sigma] \quad (4.7)$$

in which subscripts L.N.σ denotes linear, nonlinear and initial stress respectively. The plate or plate assemblies have prebuckling deformations due to initial imperfections and residual stresses before buckling occurs and these deformations may have considerable effects on the buckling stress and the mode shape of the structural members. To include the prebuckling deformations, buckling formulation can be expressed as

$$([K_T(d_0)]-[K_G(\lambda)])\{d\}=0 \quad (4.8a)$$

where $[K_G(\lambda)]$ is nonlinearly dependent on the prebuckling deformations due to the applied load and $[K_T(d_0)]$ is dependent on the initial deformations, where buckling analysis needs to start

and is expressed as

$$[K_T(d_0)]=[K_L]+[K_N(d_0)]+[K_\sigma(d_0)] \tag{4.8b}$$

$[K_G(\lambda)]$ in Eq. 4.8(a) is the change in the tangent stiffness matrix induced from the prebuckling deformations due to the applied compressive load. It is composed of two parts as

$$[K_G(\lambda)]=[K_N(d_p)]+[K_\sigma(d_p)] \tag{4.8c}$$

where $[K_\sigma(d_p)]$ is the increment of the stability matrix due to applied load level and is expressed as

$$[K_\sigma(d_p)]=\int_v [G]^T[\Delta\sigma][G]dv \tag{4.8d}$$

and $[K_N(d_p)]$ is the increment of the nonlinear tangent stiffness matrix due to prebuckling deformations and can be expressed as Eq. 4.8(e).

$$\begin{aligned}[K_N(d_p)]=&\int_v [B_L]^T[D][B_N(d_p)]dv\\&+\int_v [B_N(d_p)]^T[D][B_L]dv\\&+\int_v [B_N(d_0)]^T[D][B_N(d_p)]dv\\&+\int_v [B_N(d_p)]^T[D][B_N(d_0)]dv\\&+\int_v [B_N(d_p)]^T[D][B_N(d_p)]dv\end{aligned} \tag{4.8e}$$

in which $\mathbf{d}_0$ and $\mathbf{d}_p$ indicate initial imperfections and prebuckling deformations respectively. The lowest eigen value λ of Eq. 4.8(a) is the load factor for the buckling of sections. The Eq. 4.8(a) is a nonlinear function of the load factor λ. However, there is few efficient nonlinear algorithm available for the solution of nonlinear eigen value problems. Therefore linear eigen value solving method is carried out iteratively until the eigen value converges with certain accuracy.

5. Numerical Examples

5.1 Welded Box Sections Subjected to Uniform Compression

Welded box sections with residual stresses are loaded by uniform compression. Details of the section geomeries are shown in Fig. 6, and the test results can

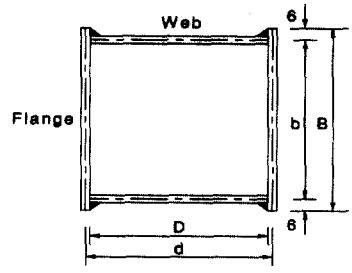

(a) Unstiffened Section

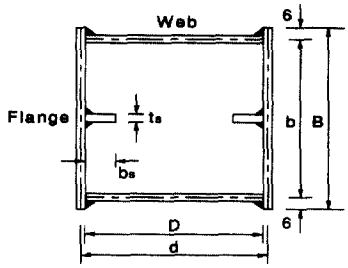

(b) Longitudinally Stiffened Section

Fig. 6 Welded Box Sections

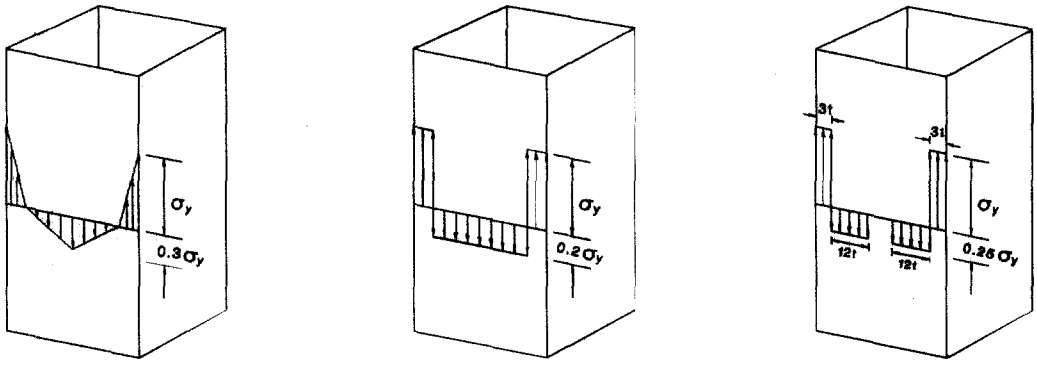

(a) case 1 (b) case 2 (c) case 3

Fig 7. Assumptions of Residual Stress Distribution

be refered to Song and Kwon(1997).

The residual stress distribution in steel plate panels due to welding were not exactly defined(Kim and Kwon 1994, Ge and Usami 1994). In this study, three types of residual stress distribution were assumed as Fig. 7 to conduct the inelastic buckling analysis and compare with the test results. For the both type of sections, it was observed that the inelastic local buckling of the plate panels occured and shaped three half-waves along overall length of the columns since aspect ratio a/b equals 3.0 and the longitudinal stiffener has the enough flexural strength to resist the distortional buckling.

The initial imperfections are neglected due to the small magnitude. However, the residual stress distribution has a significant effect on the inelastic buckling stress. Among the assumptions of residual stress distribution, case 2 seems to produce more accurate results than the others. The results are compared in Table. 1 and 2. The results show that the residual stress distribution can be assumed accurately by the tendon theory. Bi-linear properties can produce more comparative expectations for the buckling stress than Ramberg-Osgood and Plank

Table. 1 Comparison of Unstiffened Sections

Specimen	Test (MPa)	Elastic Buckling Analysis (MPa)	Inelastic Buckling Stress (MPa)						
			Plank	Ramberg-Osgood		Elastic-Perfectly Plastic			
			case 3	case 2	case 3	without residual stress	case 1	case 2	case 3
US 9	257.0	481.0	276.7	229.0	221.1	290.0	290.0	290.0	290.0
US 12	229.0	266.0	249.7	211.3	207.5	266.3	214.0	231.7	235.8
US 15	129.0	148.0	129.4	133.5	134.7	148.6	95.8	133.5	134.7

Table. 2 Comparison of Stiffened Sections

Specimen	Test (MPa)	Elastic Buckling Analysis (MPa)	Inelastic Buckling Stress (MPa)					
			Plank		Ramberg-Osgood		Elastic-Perfectly Plastic	
			case 2	case 3	case 2	case 3	case 2	case 3
SS15(35)	164.0	197.5	153.0	161.7	167.1	177.9	169.2	178.1
SS15(45)	170.0	197.6	153.3	162.0	167.3	178.2	169.4	178.4

formulas due to the characteristics of mild steel. And the numerical results obtained by the program seem to be reasonable in comparison with the test results.

5.2 Rectangular Plate Subjected to Uniform Compression

A simply supported rectangular plate with small initial imperfections is assumed to be compressed by uniform stress as shown in Fig. 8.

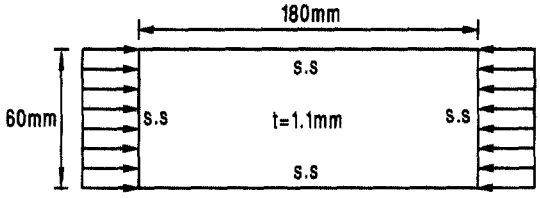

Fig. 8 Rectangular Plate Subjected to Uniform Compression

The assumed initial imperfection mode is one half-wave buckling mode which is fourth mode while the plate buckles in three half-waves which is the first buckling mode as shown in Table. 3. The imperfect plate is buckled in the first mode since the first buckling stress is well smaller than those of the second or higher buckling modes as shown in Table 3. However, if the first several buckling modes are similar or nearly similar, the imperfect plate may not buckle in the first buckling mode but may buckle in the other modes. The results obtained without considering prebuckling deformations are compared with those computed with including prebuckling deformations in Table 4. The results show that the initial imperfections increase the buckling stress

Table. 3 Buckling Mode and Stress of Perfect Plate

Buckling Mode	Buckling Stress (MPa)	Mode Shape	$\frac{\text{Width}}{\text{Half}-\text{Wavelength}}$
1st	249.1	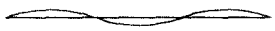	1.0
2nd	320.9		1.67
3rd	483.5		2.33
4th	692.0	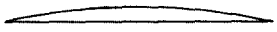	0.33

Table. 4 Buckling Stress for Rectangular Sections

Imperfections	Elastic Buckling Stress (MPa)		Inelastic Buckling Stress (MPa)	
	with Prebuckling Deformations	without Prebuckling Deformations	with Prebuckling Deformations	without Prebuckling Deformations
0.0t	249.4	249.4	220.3	220.3
0.1t	251.0	250.4	221.4	220.9
0.2t	255.6	253.2	224.2	222.5
0.3t	263.0	257.8	228.6	225.1
0.4t	272.7	264.0	234.2	228.7
0.5t	283.9	271.3	241.1	232.8
1.0t	345.9	315.8	288.6	260.1

nonlinearly as the magnitude is increased.

The buckling stress calculated excluding prebuckling deformations gives more conservative results as the magnitude of the initial imperfection is increased and can be acceptable in engineering accuracy. However, if the magnitude of the initial imperfection is considerably large, excluding the prebuckling deformations in calculation of the buckling stress may produce too conservative buckling stress. Ramberg-Osgood formula was used for the nonlinear stress strain relation.

The values of $\sigma_{0.7}$ and $\sigma_{0.85}$ were assumed as 282 MPa and 246.5 MPa respectively. The Young's modulus E was taken as 2.05×105 MPa and the yield stress σ_y was 320 MPa.

5.3 Cold-Formed Channel Sections Subjected to Uniform Compression

A lipped channel section, which has initial imperfections but are not in the clear buckling modes, is compressed with fixed boundary conditions at both ends.

Table. 5 Buckling Stress for Channel Sections

Length (mm)	Test Result		Classical Analysis		Spline Method		
	stress (MPa)	Buckling mode	stress (MPa)	Buckling mode	Initial imperfection	stress (MPa)	Buckling mode
400	89.0	D(1)+L(3)	81.5	D(1)+L(3)	0.2t	83.6	D(1)+L(3)
					0.5t	90.8	D(1)+L(3)
600	82.6	D(1)+L(5)	77.4	D(1)	0.5t	81.0	D(1)
800	74.2	D(2)+L(5)	75.5	D(1)	0.5t	75.4	D(1)
			79.4	D(1)+L(7)	1.0t	79.1	D(1)+L(7)

The geometries are given on Fig. 9. The assumed initial imperfected mode is one half-wave distortional buckling mode as shown in Fig. 9 and the maximum magnitude of the lip of the channel section at mid-length is ranged from 0.2 times thickness to 1.0 times thickness.

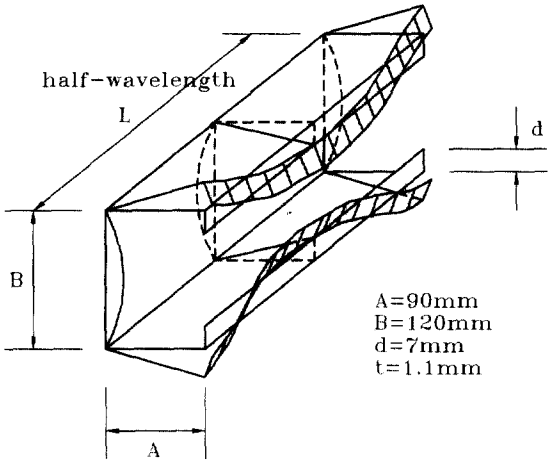

Fig. 9 Distortionally Buckled Lipped Channel

The results calculated by proposed method are compared in the Table. 8 with the test results and those obtained by classical linear buckling analysis. D and L indicate Distortional and Local buckling mode respectively and D+L indicates the mixed buckling mode. The values in parantheses indicate the number of half-wavelengths. The results show that the classical solutions are slightly conservative values compared with test results. The advanced procedure produces more accurate results since the initial imperfections and prebuckling deformations increase the buckling stress slightly.

6. Conclusion

The elastic and inelastic linearized spline finite strip buckling analysis has been developed to include the prebuckling deformations of prismatic thin-walled structures with initial imperfections and residual stresses under arbitrary loading conditions. The nonlinear stress-strain relations due to residual stress and material nonlinearity have been included.

The examples indicate that the method is efficient for analyzing the buckling response of flat plate assemblies with prebuckling deformations which may buckle into one or several half-waves and in different mode shapes. The nonlinear stress-strain relations and residual stress models used in this paper can produce resonable results in comparison with test results.

The present method is expected to account for the change of buckling modes which may occur in the post-buckling range near the second or higher bifurcation point.

감사의 말

본 논문은 1995-96년도 한국과학재단 핵심연구지원사업(No. 951-1204-016-2)의 지원으로 수행되었으며 이에 감사드립니다.

References

(1) Bijlaard, P. P (1949). "Theory and Tests on the Plastic Stability of Plates and Shells". Journal of the Aeronautical

Sciences, Vol. 16, pp. 529-541.
(2) Carl de Boor (1978). A Practical Guide to Splines. Applied Mathmatic Science, Vol.27.
(3) Fan, S. C (1982). Spline Finite Strip Method in Structural Analysis. PhD. Thesis, University of Hong Kong, Hong Kong.
(4) Ge, H. and Usami, T. (1994). Development of Earthquake-Resistant Ultimate Strength Design Method for Concrete-Filled Steel Structures. NUCE Research Report No. 9401, Nagoya University, Japan.
(5) Hancock, G. J (1978). "Local, Distortional and Lateral Buckling of I-Beams", Journal of the Structural Division, ASCE, Vol.104, No.ST11, pp. 1787-1798.
(6) Handelman, G. H and Prager, W (1948). "Plastic Buckling of a Rectangular Plate", Technical Note, NACA, No. 1530.
(7) Kim, U. S and Kwon, Y. B (1994). "A Study on the Residual Stress of H and Box Sections", Proceedings, Korean Society of Steel Constructions, pp95-103.
(8) Kwon, Y. B and Hancock, G. J (1993). "Post-Buckling Behaviour of Thin-Walled Sections Undergoing Local and Distortional Buckling", Computers and Structures, Vol, 49(3), pp. 507-516.
(9) Lau, S. C. W and Hancock, G. J (1990). "Inelastic Buckling of Channel Columns in the Distortional Mode", Thin-Walled Structures, Vol. 10, pp. 59-84.
(10) Novozhilov, V. V (1953). Foundation of the Nonlinear Theory of Elasticity. Graylock Press, Rochester, New York.
(11) Pi, Y. L and Trahair, N. S (1992). "Prebuckling Deflections and Lateral Buckling - Theory and Applications", Journal of Structural Engineering, ASCE, 118(11), pp. 2949-2985.
(12) Plank, R. J and Wittrick, W. H (1974). "Buckling under Combined Loading of Thin Flat-Walled Structures by a Complex Finite Strip Method", International Journal for Numerical Methods in Engineering, Vol. 8, No. 2, pp. 323-339.
(13) Ramberg, W and Osgood, W. R (1943). "Description of Stress-Strain Curves by Three-Parameters", Technical Note, NACA, No. 902.
(14) Song, J. Y and Kwon, Y. B (1997). "Structural Behavior of Concrete Filled Steel Box Sections", Proceding, International Conference on Composite Construction, Insbruck, Austria. pp. 795-800
(15) Zienkiewicz, O. C (1989). The Finite Element Method. Vols 1 & 2, 4th Edition, McGraw-Hill, London.

(접수일자 : 1998년 5월 18일)